

Color-color Relations for Red Giants in Star Clusters

Kaspar von Braun, Kristin Chiboucas, Jocelyn Kelly Minske, José Francisco Salgado
University of Michigan

and

Guy Worthey
St. Ambrose University

ABSTRACT

New Johnson-Cousins *UBVRI* photometry of giants in globular clusters is combined with *JHK* photometry on the CIT system to produce color sequences for giants from the globular clusters M3, M5, M13, and M92. *UBVRI* data are also presented for giants in the metal-rich open cluster NGC 6791. These data fill a gap in the literature, especially for the *R* & *I* bands. We provide the empirical relations between broad band colors for various [Fe/H] values for metal-poor giants. The color sequences for $U - B$ and $B - V$ show clear separations for different [Fe/H] values. We also find weak, though unexpected, metallicity dependences of $V - R$, $V - I$, and $J - K$ colors. $H - K$ is metal-insensitive. The above colors are plotted as a function of $V - K$, and a literature $(V - K) - T_{\text{eff}}$ relation is given.

Subject headings: globular clusters: individual (M3, M5, M13, M92), open clusters: individual (NGC 6791), stars: fundamental parameters (color, metallicity), stars: Population II

1. Introduction

Population synthesis models and stellar evolutionary isochrones are the tools which give age estimates for galaxies and star clusters, thus providing a constraint on the age of the universe. The models, however, are dependent upon the transformations from effective temperature (T_{eff}), surface gravity, and abundance to observed colors and magnitudes. In the case of metal-poor giants, these transformations remain inconclusive, despite considerable efforts in the past.

In 1966, Johnson¹ produced a remarkable set of tables that gives color-color sequences in *UBVRIJKLMN* passbands for local dwarfs, giants, and supergiants (of nearly solar metallicity, since metal-poor stars are rare in the disk), based on his and his collaborators' extensive photometry efforts. He calculated the absolute flux in each passband to obtain bolometric corrections and effective temperatures. For giants, this temperature scale has been subsequently revised (Dyck et al. 1996; DiBenedetto 1993; Ridgway et al. 1980) but the color-color sequences are still used in many contexts, including assigning colors to theoretical isochrones and computing colors for integrated light population models. Since 1966, new passbands have become standard for broadband photometry. These are the Cousins (1980a,b) *R* and *I* filters at roughly $0.68\mu\text{m}$ and $0.79\mu\text{m}$, and the CIT (Elias et al. 1982; "CIT" stands for California Institute of Technology) *H* filter at $1.6\mu\text{m}$. With these new filters, it is clear that more comprehensive color-color tables are necessary.

¹Johnson, H. L. 1966, ARA&A, 4, 193

One powerful way to generate a complete color-color table is to compute theoretical line-blanketed stellar spectra and convolve them with filter response functions to synthesize colors (e.g. Buser & Kurucz 1979; Bell & Gustafsson 1978, 1989; Kurucz 1992). The only major detriment to this approach is that, owing to the complexity of the problems of opacity and convection, the theoretical fluxes match imperfectly with real stellar fluxes. Systematic color drifts can be seen when theoretical results are compared to an empirical color-color table (cf. Worthey 1994).

Empirical tables are therefore of primary interest, for use by themselves or for use as a check of the theoretical color calibrations. The most complete empirical calibration attempted to date was done by Green (1988) for use in the Revised Yale Isochrones (Green et al. 1987). For Green’s work, solar neighborhood *UBVRI* photometry was assembled, and a temperature scale was attached via the $R - I$ color. The extension to different metallicities was accomplished by using theoretical color results. The Green calibration is imperfect; while problems with fitting isochrones (Corbally 1996) may be due to the temperature of the evolutionary tracks rather than the color calibration, the Green colors differ from other literature calibrations (Worthey 1994). A problem with bolometric corrections (Tiede, Frogel, & Terndrup 1995; Mould 1992) has also been noticed, but the color calibration has not yet been redone.

As part of an effort to redo this color calibration, a literature search conducted by Worthey and Fisher (1996) discovered a paucity of observations in the R and I passbands for metal-poor giants. New observations at the Michigan-Dartmouth-MIT (MDM) Observatory were proposed to help fill this RI gap and to provide empirical relations between the various colors for different metallicities. We selected globular clusters of known metallicity, with previous BV (and sometimes U) photometry, and specifically stars observed in JHK by Frogel et al. (1983) and Cohen et al. (1978). In order to extend the metallicity range of our data to higher $[Fe/H]$ values, NGC 6791 was added to the list. Unreduced JHK photometry exists and, we expect, will soon be available to complete the color sequence for this cluster. The approach in this paper is to concentrate *only* on the Frogel et al. (1983) and Cohen et al. (1978) stars in the globular clusters and on NGC 6791 giants previously studied by Garnavich et al. (1994). In this way, we reduce a daunting array of data to a manageable size while retaining full ability to construct $UBVRIJHK$ color sequences from the results.

We describe the observations and data reduction in the next section. In section 3.1, we give our photometry results and, in section 3.2, compare them with data found in the literature. Section 3.3 contains a discussion of the empirical color-color relations for the metal-poor giants. Section 4 contains concluding remarks.

2. Observations and Data Reduction

The observations were obtained during the nights of April 11, 12, and 13, 1997, at the MDM Observatory McGraw-Hill 1.3m telescope. A Schott glass *UBVRI* filter set fabricated to match the Johnson-Cousins system was used with a UV-coated Tek 1024 CCD. Landolt (1992) standard stars were regularly observed along with fields that were chosen to overlap previous Frogel et al. (1983) and Cohen et al. (1978) JHK target stars in globular clusters, and Garnavich et al. (1994) red giants in open cluster NGC 6791.

The initial processing of the raw CCD images was done with the routines in the IRAF² CCDPROC

²IRAF is distributed by the National Optical Astronomy Observatories, which are operated by the Association of Universities

package. For each of the three nights, 10 biases were combined for the bias subtraction. The flats were produced by combining between 3 and 6 twilight flat images per night per filter.

The processed data were reduced using DoPHOT (Schechter et al. 1993). Because the point spread function (PSF) of the stars varied with position on the CCD, we adjusted the values of some of the input parameters of DoPHOT to obtain accurate photometry results. In particular, we used the variable PSF feature of DoPHOT and, in some cases, lowered DoPHOT’s sensitivity with respect to detecting nearby neighbors of stars. The latter was done in order to avoid false multiple detections of individual, slightly elongated stellar images.

DoPHOT’s photometry output contains a list of aperture corrections for stars with small photometric errors and without nearby neighbors. In order to apply the correct aperture correction for each of our target stars, we selected from this list the stars far away from the cluster, so as to avoid aperture corrections influenced by the higher sky value in the immediate vicinity of the cluster. With the fairly large field of view of the CCD, this method left us with between roughly 10 and 240 isolated stars with high S/N ratios for the various images. Using these stars, the dependence (if any) of the aperture correction upon position on the CCD was determined, using a linear fit in x and y . The F-test (cf. Press et al. 1992) was used to determine if fits which included x - and y -terms were statistically different from a constant value for the aperture correction applied over the whole chip.

During our three photometric nights, we observed a total of 10 Landolt (1992) fields, at airmass values ranging from ~ 1.15 to ~ 1.55 . Using the IRAF PHOTCAL package, we applied standard star solutions for all three nights of the form

$$V = v + a_0 + b_0 X_v + c_0(b - v) \tag{1}$$

$$B - V = a_1 + b_1 X_b + c_1(b - v) \tag{2}$$

$$U - B = a_2 + b_2 X_u + c_2(u - b) \tag{3}$$

$$V - R = a_3 + b_3 X_r + c_3(v - r) \tag{4}$$

$$V - I = a_4 + b_4 X_i + c_4(v - i), \tag{5}$$

where the a_j , b_j , and c_j are the fitted constants, X_{filter} is the airmass of the exposure taken with the respective filter, the lowercase magnitudes are instrumental, and the uppercase ones are the final calibrated magnitudes.

The RMS errors for the fits for the three nights are given in Table 1, and the residuals between the calculated magnitudes and the ones given by Landolt (1992) are plotted in Fig. 1.

Roughly two-thirds of the program stars were observed only on one night (usually 3 CCD frames per filter, 2 frames for the U filter), but about one-third of the stars were observed on two nights. For all the stars, the V magnitudes and colors were averaged arithmetically.

The photometric scatter between nights 2 and 3, based on 8 stars in NGC 6791, is around 0.01 mag for VRI and about 0.015 mag for UBV colors. With only 8 stars, the estimated error of our photometry for these nights is the photometric scatter divided by $\sqrt{8}$, which is around 0.004 mag and 0.005 mag for VRI

and UBV colors, respectively. These values are consistent with the RMS of the standard star solutions (Table 1).

However, for 7 globular cluster stars in common between nights 1 and 2, the colors matched to a photometric scatter of 0.03 mag for all colors, significantly larger than what the standard star solutions imply. The $B - V$ colors for these stars were also systematically different by 0.05 mag. For these reasons, night 1 data were dropped whenever possible. Only two stars were observed in night 1 alone, and these are marked in Table 2.

3. Results and Discussion

3.1. Photometry Results

Reduced magnitudes and errors for our program giants (luminosity class 3) are given in Table 2. The “Err1” column gives a magnitude error estimate based on the number of observations and the scatter between individual measurements. The error is quantized in 0.005-mag steps. Colors involving the U filter should be assumed to have 50% larger errors than the “Err1” entry would suggest. The “Err2” column contains an entry if one or more filters had few observations or if there was extra scatter between measurements. For instance, an entry of “.03ui” means that any color involving U or I should be considered to have an error of 0.03 mag.

Table 3 contains the dereddened (via Cardelli et al. 1989) photometry results. Star identifications are given along with $[\text{Fe}/\text{H}]$ and $E(B - V)$ from Harris (1996). Infrared photometry is from Cohen et al. (1978) and Frogel et al. (1983). Their raw photometry results were used, also dereddened using Cardelli et al. (1989). This allows full $UBVR IJHK$ color sequences to be constructed.

3.2. Literature Comparison

We conducted a literature search to compare our photometry to previous studies whenever possible. For $U - B$, we found 20 globular cluster stars in common with pre-1975 photometry (no more recent data were discovered). The median $\delta(U - B) = (U - B)_{\text{this work}} - (U - B)_{\text{literature}}$ is -0.08 . By contrast, three NGC 6791 stars in common with Harris & Canterna (1981) compare with $\delta(U - B) = +0.14$. It thus seemed that $\delta(U - B)$ increased with increasing $[\text{Fe}/\text{H}]$ values, and we considered various filter defects that could generate this metallicity trend. However, the behavior is counter to that expected from a red leak, and the UV coating on the CCD should make the overall U filter response fairly similar to the original, so we believe that we have approximated the Landolt standard system very well, as implied by the standard star solutions.

The other colors did not display such a trend. Literature $B - V$ values were found for 42 program stars (Cathey (1974); Arp (1955); Arp (1962); Kaluzny (1993, private communication); Cudworth (1995, private communication); Harris & Canterna (1981); Kinman (1965); Kaluzny & Rucinski (1995)), and the overall average $\delta(B - V) = -0.03$. Concentrating on the most recent data, the three NGC 6791 stars in common with Harris & Canterna (1981) give $\delta(B - V) = +0.007$, and the three stars in common with Kaluzny & Rucinski (1995) give $\delta(B - V) = +0.015$. VI photometry of 13 NGC 6791 stars in common with Garnavich et al. (1994) yields an average $\delta(V - I) = -0.15$ mag, but we are less concerned with this offset because of the relatively low accuracy of 0.05 mag claimed by these authors.

3.3. Discussion

The major goal of this study is to explicitly reveal the metallicity dependence of broad-band colors. For instance, $(U - B)_0$ has long been used to estimate the metallicity of faint stars (e.g. van den Bergh 1962). Figures 2, 3, 4, 5, 6, and 7 show the various dereddened colors versus $(V - K)_0$ for giants of widely differing metal abundances, including the globular cluster giants from this work. $(V - K)_0$ is chosen because it is an excellent temperature indicator for GKM giants, with a large color range compared to its observational uncertainty. In addition, the best model fluxes show no metallicity sensitivity. That is, one temperature - $(V - K)_0$ conversion is applicable to stars of all abundances, at least in the 4000K to 5000K range (e.g. Bessell et al. 1989, 1991; Kurucz 1992; Bell & Gustafsson 1989).

A fit to the effective temperature — $(V - K)_0$ relation of Ridgway et al. (1980) is

$$(V - K)_0 = 34.19 - 0.01520T + 2.420 \times 10^{-6}T^2 - 1.330 \times 10^{-10}T^3, \quad (6)$$

where T is T_{eff} in degrees Kelvin. The range is valid over $1.5 < (V - K)_0 < 4$, or $3800 < T_{\text{eff}} < 5600$ K. This approximate formula is given as a convenience for readers, but they should be aware that the cubic curve can deviate from the Ridgway et al. calibration by as much as about 0.08 mag in $(V - K)_0$, which corresponds to about 60 K in effective temperature. Serious users may want to refer to the original temperature calibration table.

Our photometry plus the Worthey & Fisher (1996) literature photometry, all dereddened, produced relations summarized here as six formulae giving colors as a function of $(V - K)_0$ and $[\text{Fe}/\text{H}]$. Much of the literature photometry comes from the machine readable version of Morel & Magnenat (1978) and is on the Johnson system. The RI data were transformed using the relations given by M. S. Bessell (1979). $[\text{Fe}/\text{H}]$ values were obtained from McWilliam (1990) and Cayrel de Strobel et al. (1992). The fits below are non-linear least-squares regressions as described by Press et al. (1992). Some data were rejected in a $2.5\text{-}\sigma$ rejection loop, but never more than a few percent were discarded. Most of the literature data are photographic with quoted error of $\sim 5\%$, whereas the data of this work have errors more on the order of $\sim 2\%$. Consequently, we included a weighting factor of ~ 2.8 to our data. This value is derived from the conservative estimate that our errors are up to 60% of the literature errors. Theoretical colors from Worthey (1994) were included at low statistical weight ($\frac{1}{4}$ of the literature datapoints) to provide guidance in regions with no stars. These 48 “stars” are included in the total N (number of datapoints) below, except for the $(V - I)_0$ equation (theory data produce a large range in V-I for a given V-K which is not reflected in observational data). Different combinations of coefficients were compared using the F-test and only statistically significant terms were retained. The fits are good *only* in the regime $1.6 < (V - K)_0 < 3.6$, but cover the range of Galactic $[\text{Fe}/\text{H}]$ values for giants. Note that, although we omit stars with $-1 < [\text{Fe}/\text{H}] < 0$ in the plots for the sake of clarity, all metallicities are included in the derivation of the fits.

$$\begin{aligned} (U - B)_0 &= -1.0121 + 0.8239 (V - K)_0 + 0.04431 [\text{Fe}/\text{H}]^2 \\ &+ 0.3752 (V - K)_0 [\text{Fe}/\text{H}] - 0.0868 (V - K)_0^2 [\text{Fe}/\text{H}]; \\ &(N = 428, RMS = 0.082) \end{aligned} \quad (7)$$

$$\begin{aligned} (B - V)_0 &= 0.1116 + 0.4013 (V - K)_0 + 0.3509 [\text{Fe}/\text{H}] \\ &- 0.0823 (V - K)_0 [\text{Fe}/\text{H}] + 0.01298 (V - K)_0 [\text{Fe}/\text{H}]^2; \\ &(N = 625, RMS = 0.062) \end{aligned} \quad (8)$$

$$(V - R)_0 = -0.0040 + 0.2271 (V - K)_0 + 0.0100 [\text{Fe}/\text{H}]; \quad (9)$$

$(N = 301, \text{RMS} = 0.021)$

$$(V - I)_0 = 0.1595 + 0.3387 (V - K)_0 + 0.004291 (V - K)_0^3 \\ + 0.004255 (V - K)_0^2 [\text{Fe}/\text{H}] - 0.005596 [\text{Fe}/\text{H}]^3; \quad (10)$$

$(N = 267, \text{RMS} = 0.026)$

$$(J - K)_0 = 0.0231 + 0.2613 (V - K)_0 + 0.009869 (V - K)_0 [\text{Fe}/\text{H}]; \quad (11)$$

$(N = 642, \text{RMS} = 0.029)$

$$(H - K)_0 = -0.0190 + 0.04402 (V - K)_0; \quad (12)$$

$(N = 446, \text{RMS} = 0.020)$

The $(V - R)_0$ fit contains an $[\text{Fe}/\text{H}]$ term that is statistically significant, but only at the 50% level. The real behavior of $(V - R)_0$ is probably more subtle than the simple fit can reproduce. The $(J - K)_0$ color equation contains a very significant $(V - K)_0[\text{Fe}/\text{H}]$ term. This indicates a metallicity dependence of the $(J - K)_0$ color, which is usually assumed to be a pure temperature indicator. Fitting the $(V - I)_0$ data produced a somewhat surprising result. At first glance, one might assume that the data may be well represented by a metallicity-independent, linear fit in $(V - K)_0$ (see Fig. 5). We find, however, a more complex behavior with respect to both metallicity and $(V - K)_0$. The functional dependence of $(V - I)_0$ upon $[\text{Fe}/\text{H}]$ is weak, but significant.

There is a possibility that an error in the assumed $E(B - V)$ values of the various clusters could affect the fitting results. We investigated the effect an $E(B - V)$ error of ± 0.02 would have on datapoints but found that the resulting shifts in color are small compared to the spread due to different metallicities. In order to demonstrate the magnitude and direction of the shift of the datapoints in the color-color diagrams due to a reddening error, we provide the reddening vectors for $E(B - V) = 0.10$ (see Figures 2 through 7). This value is, of course, far beyond a reasonable error in $E(B - V)$, but lower values produced vectors which were too small to be visible in the figures. The vectors were created using the reddening curve by Cardelli et al. (1989).

Our photometry is good enough to show separation of $(U - B)_0$ sequences for globular clusters of differing metallicities in Figure 2. M92 stars (at $[\text{Fe}/\text{H}] = -2.29$)³ lie to numerically smaller (i.e., bluer) $(U - B)_0$ from the other globular clusters. There is also a hint that M3 ($[\text{Fe}/\text{H}] = -1.57$) and M13 stars ($[\text{Fe}/\text{H}] = -1.54$) lie blueward of M5 ($[\text{Fe}/\text{H}] = -1.29$). This illustrates the metallicity sensitivity of $(U - B)_0$ and also confirms our optimistic assessment of our photometric accuracy. Our M92 data are significantly bluer in $(U - B)_0$ than literature data of similar $[\text{Fe}/\text{H}]$ in the range $2.1 < (V - K)_0 < 2.7$. Stars in this region have higher T_{eff} and are thus fainter since they lie further toward the subgiant branch. It is likely that the discrepancy is due to the fact that the literature data are photographic, but more CCD data are needed to verify this. Included in the figure are the $(U - B)_0$ fits for several $[\text{Fe}/\text{H}]$ values.

³All globular cluster $[\text{Fe}/\text{H}]$ values are from Harris (1996).

Figure 3 also clearly displays a dependence of $(B - V)_0$ color upon $[\text{Fe}/\text{H}]$. It is interesting to note that all the fits for the various values of metallicity intersect in the region $(V - K)_0 \sim 3$. Figures 4 and 6 show a much weaker dependence of $(V - R)_0$ and $(J - K)_0$ on $[\text{Fe}/\text{H}]$, as indicated by the equations above. There is a hint that the $(V - R)_0$ sequence shows a divergence for different metallicity ranges around $2 < (V - K)_0 < 3$, but more data are needed to make sure.

The interesting behavior of $(V - I)_0$ is displayed in Figure 5. Giants with solar $[\text{Fe}/\text{H}]$ fall toward numerically lower $(V - I)_0$ values than the ones with $[\text{Fe}/\text{H}] < 2$ for $(V - K)_0 < 2.4$. At $(V - K)_0 > 2.8$, however, the solar metallicity curve lies above the ones representing the lower metallicity ranges. Furthermore, stars with $[\text{Fe}/\text{H}] = -1$ fall toward lower $(V - I)_0$ than solar $[\text{Fe}/\text{H}]$ stars throughout the range of $(V - K)_0$. Another noteworthy result is the non-linear dependence of $(V - I)_0$ on $(V - K)_0$. It is apparent from the plot that the fits approximate the datapoints very well. Since this $(V - I)_0$ behavior was unexpected, we examined the possibility of single datasets overly influencing the fit, but when the function was refit without the Walker (1994) and the da Costa & Armandroff (1990) M15 data, as well as the theoretical points, it remained unchanged. It is worth mentioning that the dependence of $(V - I)_0$ on metallicity is a significantly lower-amplitude effect than the one on $(V - K)_0$. $(V - I)_0$ therefore remains a useful color index for temperature determination.

Figure 7 shows the opposite case: $(H - K)_0$ displays no sensitivity to metal abundance. In this plot, stars of all abundances overlie the same locus. It is most likely that both colors, $(H - K)_0$ and $(V - K)_0$, have negligible metallicity sensitivity (rather than the alternative that both have measureable sensitivities, but the sensitivities conspire to look similar in the color-color plot). The $(H - K)_0$ plot has a very small range compared to its observational error.

4. Concluding Remarks

We have presented color sequences and analytical color-color fits for giants as a function of $[\text{Fe}/\text{H}]$. The well-known metallicity sensitivity of $(U - B)_0$ is clearly visible in Fig. 2. Our data underscore this high sensitivity, especially in the higher T_{eff} regime. A somewhat weaker dependence upon $[\text{Fe}/\text{H}]$ was found for $(B - V)_0$. This color shows an interesting metallicity degeneracy at $(B - V)_0 \sim 1.3$. The colors $(V - R)_0$, $(V - I)_0$, and $(J - K)_0$ are much less influenced by metallicity, while $(H - K)_0$ is solely a function of $(V - K)_0$ (and thus T_{eff}). The dependence of $(J - K)_0$ and $(V - I)_0$ on $[\text{Fe}/\text{H}]$ was a surprising result; more data would certainly be useful to confirm our findings. The extremely weak metallicity dependences of $(V - R)_0$ and $(V - I)_0$ make these viable temperature indicators, with the advantage of only requiring an optical detector as opposed to an optical/IR combination.

This research was funded in part by NASA through grant HF-1066.01-94A from the Space Telescope Science Institute, which is operated by the Association of Universities for Research in Astronomy, Inc., under NASA contract NAS5-26555. Thanks to Brent Fisher for a good deal of hard work in mining the gold out of the literature photometry ore. We would also like to thank Mario Mateo for his helpful comments regarding DoPHOT and aperture corrections. Finally, thanks to the anonymous referee for his/her insightful comments and suggestions.

REFERENCES

- Arp, H. C. 1955, *AJ*, 60, 317
- Arp, H. C. 1962, *ApJ*, 135, 311
- Bell, R. A., & Gustafsson, B. 1978, *A&AS*, 34, 229
- Bell, R. A., & Gustafsson, B. 1989, *MNRAS*, 236, 653
- Bessell, M. S. 1979, *PASP*, 91, 589
- Bessell, M. S., Brett, J. M., Scholz, M., & Wood, P. R. 1989, *A&AS*, 77, 1
- Bessell, M. S., Brett, J. M., Scholz, M., & Wood, P. R. 1991, *A&AS*, 89, 335
- Buser, R. & Kurucz, R. L. 1979, *A&A*, 70, 555
- Cardelli, J. A., Clayton, G. C., Mathis, J. S. 1989, *ApJ*, 345, 245
- Cathey, L. 1974, *AJ*, 79, 1370
- Cayrel de Strobel, G., Hauck, B., François, P., Thévenin, F., Friel, E., Mermilliod, M., and Borde, S. 1992, *A&AS*, 95, 273
- Cohen, J. C., Frogel, J. A., and Persson, S. E. 1978, *ApJ*, 222, 165
- Cousins, A. W. 1980a, *South African Astron. Obs. Circ.*, 1, 166
- Cousins, A. W. 1980b, *South African Astron. Obs. Circ.*, 1, 234
- Corbally, C. 1996, *BAAS*, 189, 78.12
- da Costa, G. S., & Armandroff, T. E. 1990, *AJ*, 100, 162
- Demarque, P., Green, E. M., and Guenther, D. B. 1992, *AJ*, 103, 151
- DiBenedetto, G. P. 1993, *A&A*, 270, 315
- Dyck, H. M., Benson, J. A., van Belle, G. T., and Ridgway, S. T. 1996, *AJ*, 111, 1705
- Elias, J. H., Frogel, J. A., Matthews, K., and Neugebauer, G. 1982, *AJ*, 87, 1029
- Friel, E. D., and Janes, K. A. 1993, *A&A*, 267, 75
- Frogel, J. A., Persson, S. E., and Cohen, J. G. 1983, *ApJS*, 53, 713
- Garnavich, P. M., Vandenberg, D. A., Zurek, D. R., and Hesser, J. E. 1994, *AJ*, 107, 1097
- Green, E. M. 1988, in *Calibration of Stellar Ages*, ed. A. G. Davis Philip (Schenectady, NY: L. Davis), 81
- Green, E. M., Demarque, P., & King, C. R. 1987, *The Revised Yale Isochrones and Luminosity Functions* (New Haven: Yale University Observatory)
- Harris, W. E., & Canterna, R. 1981, *AJ*, 86, 1332
- Harris, W. E. 1996, *AJ*, 112, 1487
- Kaluzny, J. 1990, *MNRAS*, 243, 492
- Kaluzny, J., Rucinski, S. M. 1995, *A&AS*, 114, 1
- Kinman, T. D. 1965, *ApJ*, 142, 655
- Kurucz, R. L. 1992, in *IAU Symp. 149, The Stellar Populations of Galaxies*, ed. B. Barbuy & A. Renzini (Dordrecht: Kluwer), 225
- Johnson, H. L. 1966, *ARA&A*, 4, 193

- Landolt, A. 1992, *AJ*, 104, 340
- Liebert, J., Saffer, R. A., and Green, E. M. 1994, *AJ*, 107, 1408
- McWilliam, A. 1990, *ApJS*, 74, 1075
- Morel, M., & Magnenat, P. 1978, *A&AS*, 34, 477
- Mould, J. R. 1992, in *IAU Symp. 149, The Stellar Populations of Galaxies*, ed. B. Barbuy & A. Renzini (Dordrecht: Kluwer), 181
- Press, W., Teukolsky, S., Vetterling, W., Flannery, B. 1992, *Numerical Recipes*, 2nd Edition (Cambridge University Press)
- Ridgway, S. T., Joyce, R. R., White, N. M., and Wing, R. F. 1980, *ApJ*, 235, 126
- Schechter, P. L., Mateo, M., and Saha, A. 1993, *PASP*, 105, 1342.
- Tiede, G. P., Frogel, J. A., & Terndrup, D. M. 1995, *BAAS*, 186, 50.06
- van den Bergh, S. 1962, *AJ*, 67, 486
- Walker, A. R., 1994, *AJ*, 108, 555
- Worthey, G. & Fisher, B. 1996, *BAAS*, 28, 1366, #72.05
- Worthey, G. 1994, *ApJS*, 95, 107

Table 1. Calibration RMS Errors

	V	B-V	U-B	V-R	V-I
Night 1	0.0165	0.0088	0.0254	0.0047	0.0082
Night 2	0.0166	0.0072	0.0234	0.0051	0.0052
Night 3	0.0097	0.0105	0.0187	0.0077	0.0075

Table 2. Photometry Results

Cluster	Star ID	V	U-B	B-V	V-R	V-I	Err1	Err2
M3 ^a	II-18	14.105	0.400	0.935	0.515	0.980	0.015	...
	I-21 ^c	13.075	1.150	1.340	0.700	1.355	0.030	...
	III-77	13.365	1.060	1.255	0.620	1.250	0.015	0.03u
	III-28	12.815	1.150	1.355	0.695	1.335	0.015	0.03ui
	II-46	12.755	1.455	1.510	0.770	...	0.015	0.03u
	IV-25	13.680	0.820	1.105	0.630	1.200	0.015	...
M92 ^a	IV-2 ^c	13.500	0.285	0.970	0.505	1.095	0.030	...
	IV-10	13.455	0.335	0.920	0.560	1.100	0.015	...
	IV-114	13.865	0.255	0.810	0.540	1.045	0.015	...
	III-82	13.375	0.395	0.935	0.575	1.150	0.015	...
	II-70	13.120	0.400	0.985	0.590	1.165	0.015	...
	III-4	14.155	...	0.755	0.470	0.935	0.015	...
	XI-19	12.870	0.530	1.070	0.605	1.190	0.015	0.03ui
	X-49	12.220	0.855	1.270	0.680	...	0.015	...
	VIII-43	14.615	0.070	0.750	0.485	0.970	0.015	...
	M13 ^a	I-24	12.955	0.845	1.055	0.675	1.275	0.015
I-23		13.200	0.570	0.935	0.615	1.175	0.015	...
I-18		13.950	0.465	0.855	0.590	1.115	0.015	...
I-2		14.290	0.395	0.840	0.550	1.045	0.015	...
M5 ^a	II-50	13.880	0.630	1.005	0.570	1.105	0.015	0.02v
	III-3	12.470	1.475	1.440	0.770	1.450	0.015	...
	III-16	14.235	0.265	0.780	0.485	0.950	0.015	...
	III-53	13.545	0.525	0.940	0.540	1.070	0.015	...
	III-56	13.365	0.685	1.005	0.565	1.120	0.015	...
	III-78	12.650	1.320	1.380	0.730	1.400	0.015	...
	IV-19	12.610	1.320	1.380	0.715	1.375	0.015	...
	IV-3	14.955	0.285	0.810	0.520	0.990	0.015	...
	IV-28	14.395	0.550	0.945	0.520	1.025	0.015	...
	IV-86	14.970	-0.045	0.590	0.375	0.755	0.015	0.03u
	IV-81	12.280	1.725	1.580	0.830	1.545	0.015	...
	IV-47	12.425	1.510	1.430	0.755	1.430	0.015	...
	IV-59	12.690	1.200	1.280	0.665	1.255	0.015	...
	I-25	13.595	0.780	1.040	0.585	1.125	0.015	...
	I-20	12.555	1.335	1.350	0.700	1.320	0.015	...
	I-14	13.010	1.080	1.200	0.655	1.245	0.015	...
	I-68	12.500	1.510	1.430	0.750	1.420	0.015	...
	I-67	13.985	0.310	0.770	0.485	0.915	0.015	...
	I-55	13.645	0.490	0.885	0.525	1.010	0.015	...
	I-1	14.185	0.285	0.770	0.475	0.935	0.015	...
	II-9	12.595	1.335	1.350	0.715	1.370	0.015	0.03v

Table 2—Continued

Cluster	Star ID	V	U-B	B-V	V-R	V-I	Err1	Err2
NGC 6791 ^b	R17	14.575	1.770	1.530	0.800	1.510	0.010	...
	R4	14.000	1.415	1.580	1.355	...	0.010	0.015r
	R19	14.140	1.975	1.630	0.895	1.740	0.010	...
	R23	14.875	1.520	1.385	0.700	1.305	0.010	...
	R9	14.130	1.985	1.595	0.885	1.705	0.010	...
	R24	14.980	1.750	1.450	0.785	1.460	0.010	...
	R22	14.525	1.580	1.390	0.710	1.355	0.015	...
	R12	13.835	2.040	1.650	0.930	1.920	0.010	0.015r
	R11	14.600	1.765	1.500	0.775	1.475	0.010	0.02b
	R3	14.070	2.220	1.710	0.965	1.940	0.015	0.03u
	R21	14.720	1.700	1.470	0.770	1.445	0.015	0.03u
	R25	14.715	1.490	1.395	0.715	1.340	0.015	...
	R10	14.570	1.765	1.585	0.800	1.540	0.015	...
	R16	13.740	2.055	1.635	0.865	1.730	0.015	...

^aThe star IDs follow the numbering scheme used by Cohen et al. (1978).

^bThe star IDs follow the numbering scheme used by Garnavich et al. (1994).

^cThese stars were only observed during night 1.

Note. — All values in this table are rounded to the nearest 0.005.

Table 3. Photometry Results - Dereddened

Cluster	Star ID	[Fe/H] ^{1,2}	E_{B-V} ^{1,3}	V	U-B	B-V	V-R	V-I	V-K	K	J-K	H-K
M3	II-18	-1.57	0.01	14.075	0.393	0.925	0.508	0.965	2.348	11.727	0.645	0.088
	I-21			13.045	1.143	1.330	0.693	1.340	3.098	9.947	0.795	0.088
	III-77			13.335	1.053	1.245	0.613	1.235	3.008	10.327	0.795	0.118
	III-28			12.785	1.143	1.345	0.688	1.320	3.188	9.597	0.815	0.098
	II-46			12.725	1.448	1.500	0.763	...	3.478	9.247	0.875	0.108
	IV-25			13.650	0.813	1.095	0.628	1.185	2.873	10.777	0.765	0.128
M92	IV-2	-2.29	0.02	13.440	0.271	0.950	0.490	1.065	2.417	11.023	0.630	0.085
	IV-10			13.395	0.321	0.900	0.545	1.070	2.522	10.873	0.620	0.095
	IV-114			13.805	0.241	0.790	0.525	1.015	2.392	11.413	0.590	0.075
	III-82			13.315	0.381	0.915	0.560	1.120	2.532	10.783	0.660	0.125
	II-70			13.060	0.386	0.965	0.575	1.135	2.627	10.433	0.660	0.105
	III-4			14.095	...	0.735	0.455	0.905	2.102	11.993	0.540	0.065
	XI-19			12.810	0.516	1.050	0.590	1.160	2.657	10.153	0.690	0.095
	X-49			12.160	0.841	1.250	0.665	...	2.927	9.233	0.750	0.115
	VIII-43			14.555	0.056	0.730	0.470	0.940	2.142	12.413	0.490	0.015
M13	I-24	-1.54	0.02	12.895	0.831	1.035	0.660	1.245	2.842	10.053	0.720	0.105
	I-23			13.140	0.556	0.915	0.600	1.145	2.577	10.563	0.650	0.115
	I-18			13.890	0.451	0.835	0.575	1.085	2.477	11.413	0.640	0.105
	I-2			14.230	0.381	0.820	0.535	1.015	2.327	11.903	0.600	0.105
M5	I-1	-1.29	0.03	14.095	0.264	0.740	0.453	0.890	2.015	12.080	0.525	0.113
	I-14			12.920	1.059	1.170	0.633	1.200	2.980	9.940	0.785	0.093
	I-20			12.465	1.314	1.320	0.678	1.275	3.085	9.380	0.815	0.153
	I-25			13.505	0.759	1.010	0.563	1.080	2.675	10.830	0.705	0.113
	I-55			13.555	0.469	0.855	0.503	0.965	2.365	11.190	0.605	0.103
	I-67			13.895	0.289	0.740	0.463	0.870	2.085	11.810	0.515	0.053
	I-68			12.410	1.489	1.400	0.728	1.375	3.350	9.060	0.855	0.113
	II-9			12.505	1.314	1.320	0.693	1.325	3.215	9.290	0.825	0.103
	II-50			13.790	0.609	0.975	0.548	1.060	2.600	11.190	0.685	0.083
	III-3			12.380	1.454	1.410	0.748	1.405	3.360	9.020	0.855	0.113
	III-16			14.145	0.244	0.750	0.463	0.905	2.155	11.990	0.515	0.063
	III-53			13.455	0.504	0.910	0.518	1.025	2.405	11.050	0.625	0.093
	III-56			13.275	0.664	0.975	0.543	1.075	2.535	10.740	0.645	0.073
	III-78			12.560	1.299	1.350	0.708	1.355	3.200	9.360	0.825	0.103
	IV-3			14.865	0.264	0.780	0.498	0.945	2.155	12.710	0.565	0.073
	IV-19			12.520	1.299	1.350	0.693	1.330	3.190	9.330	0.815	0.103
	IV-28			14.305	0.529	0.915	0.498	0.980	2.455	11.850	0.645	0.123
	IV-47			12.335	1.489	1.400	0.733	1.385	3.345	8.990	0.895	0.123
	IV-59			12.600	1.179	1.250	0.643	1.210	2.950	9.650	0.755	0.083
	IV-81			12.190	1.704	1.550	0.808	1.500	3.580	8.610	0.895	0.133
IV-86			14.880	-0.066	0.560	0.353	0.710	1.630	13.250	0.365	-0.037	

Table 3—Continued

Cluster	Star ID	[Fe/H] ^{1,2}	E_{B-V} ^{1,3}	V	U-B	B-V	V-R	V-I	V-K	K	J-K	H-K
NGC 6791	R17	0.20	0.13	14.175	1.677	1.395	0.700	1.309
	R4			13.600	1.322	1.445	1.255	
	R19			13.740	1.882	1.495	0.795	1.539
	R23			14.475	1.427	1.250	0.600	1.104
	R9			13.730	1.892	1.460	0.785	1.504
	R24			14.580	1.657	1.315	0.685	1.259
	R22			14.125	1.487	1.255	0.610	1.154
	R12			13.435	1.947	1.515	0.830	1.719
	R11			14.200	1.672	1.365	0.675	1.274
	R3			13.670	2.127	1.575	0.865	1.739
	R21			14.320	1.607	1.335	0.670	1.244
	R25			14.315	1.397	1.260	0.615	1.139
	R10			14.170	1.672	1.450	0.700	1.339
	R16			13.340	1.962	1.500	0.765	1.529

¹All globular cluster data: Harris (1996).

²For NGC 6791: Friel and Janes (1993) and Garnavich et al. (1994).

³For NGC 6791: Friel and Janes (1993), Harris and Canterna (1981), and Liebert et al. (1994). We would like to note, however, that higher values for E_{B-V} were obtained by Demarque et al. (1992) and Kaluzny (1990).

Note. — The reddening calculations in this table are based on Cardelli et al. (1989).

Note. — The star numbering system used is the same as the one in Table 2.

Note. — The dereddened infrared magnitudes and colors were obtained by applying the Cardelli et al. reddening curve to observed photometry by Frogel et al. (1983) and Cohen et al. (1978). For M3, M13, and M92, Cohen et al. cite infrared photometry errors of 0.02 mag for K , $J - H$, and $H - K$. The infrared photometry errors for M5 quoted by Frogel et al. are 0.03 mag for K , $J - K$, and $H - K$.

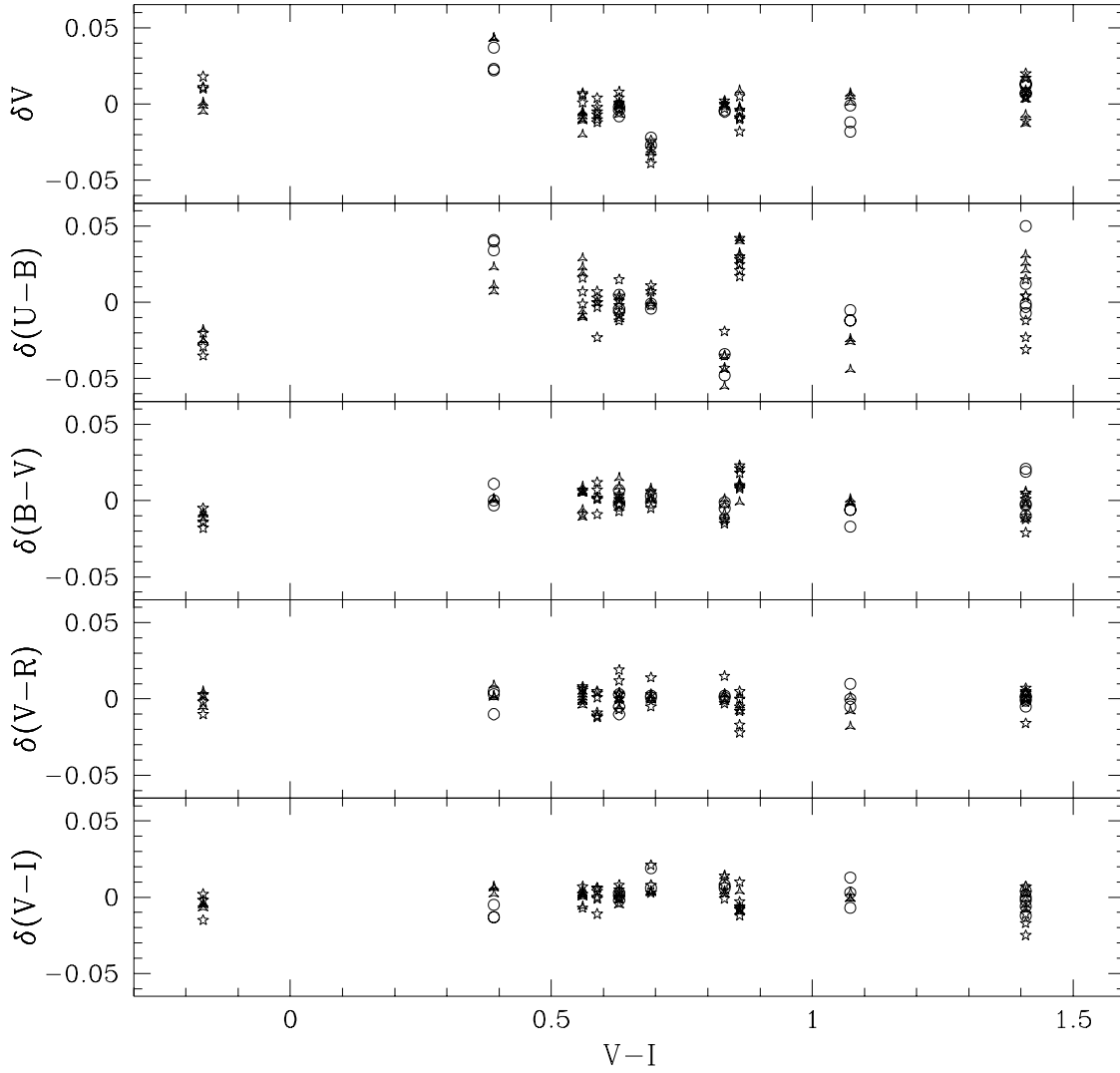


Fig. 1.— The residuals between the calculated magnitudes and standard magnitudes of the ~ 90 Landolt (1992) stars vs their standard $(V-I)$ color. Open circles, triangles, and stars represent datapoints obtained during night 1, night 2, and night 3, respectively.

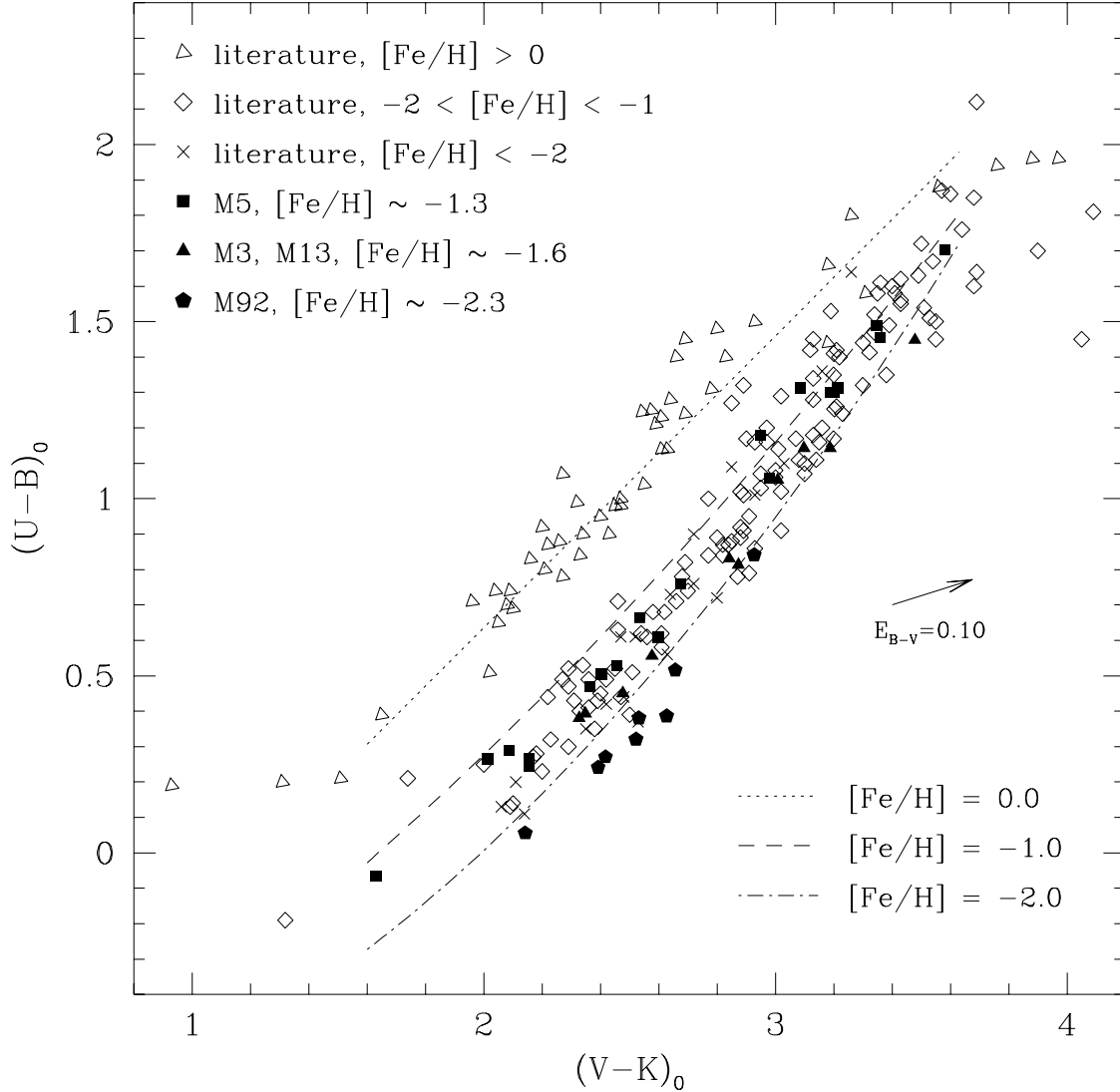


Fig. 2.— The color plane $(U - B)_0$ versus $(V - K)_0$. Program stars are marked with solid symbols as keyed. Literature data are also plotted, with different symbols for stars with $[\text{Fe}/\text{H}] > 0$, $[\text{Fe}/\text{H}] < -2$, and $[\text{Fe}/\text{H}]$ between -1 and -2 . Stars with metallicities between $[\text{Fe}/\text{H}] = 0$ and -1 have been omitted for clarity. Fits for $[\text{Fe}/\text{H}] = 0.0, -1.0, -2.0$ are superimposed for the range in which they are valid. (cf. equation (7)). The reddening vector indicates the direction along which reddening increases in this color-color plot. The length of the vector corresponds to $E(B - V) = 0.10$. The strong separation between giants of differing abundances is clearly visible. For the program stars, targets in M92, the metal-poorest cluster in this figure, lie on a sequence toward bluer $(U - B)_0$. This trend is less obvious but present in the literature collection. Sequences of all metallicities converge at the coolest temperatures.

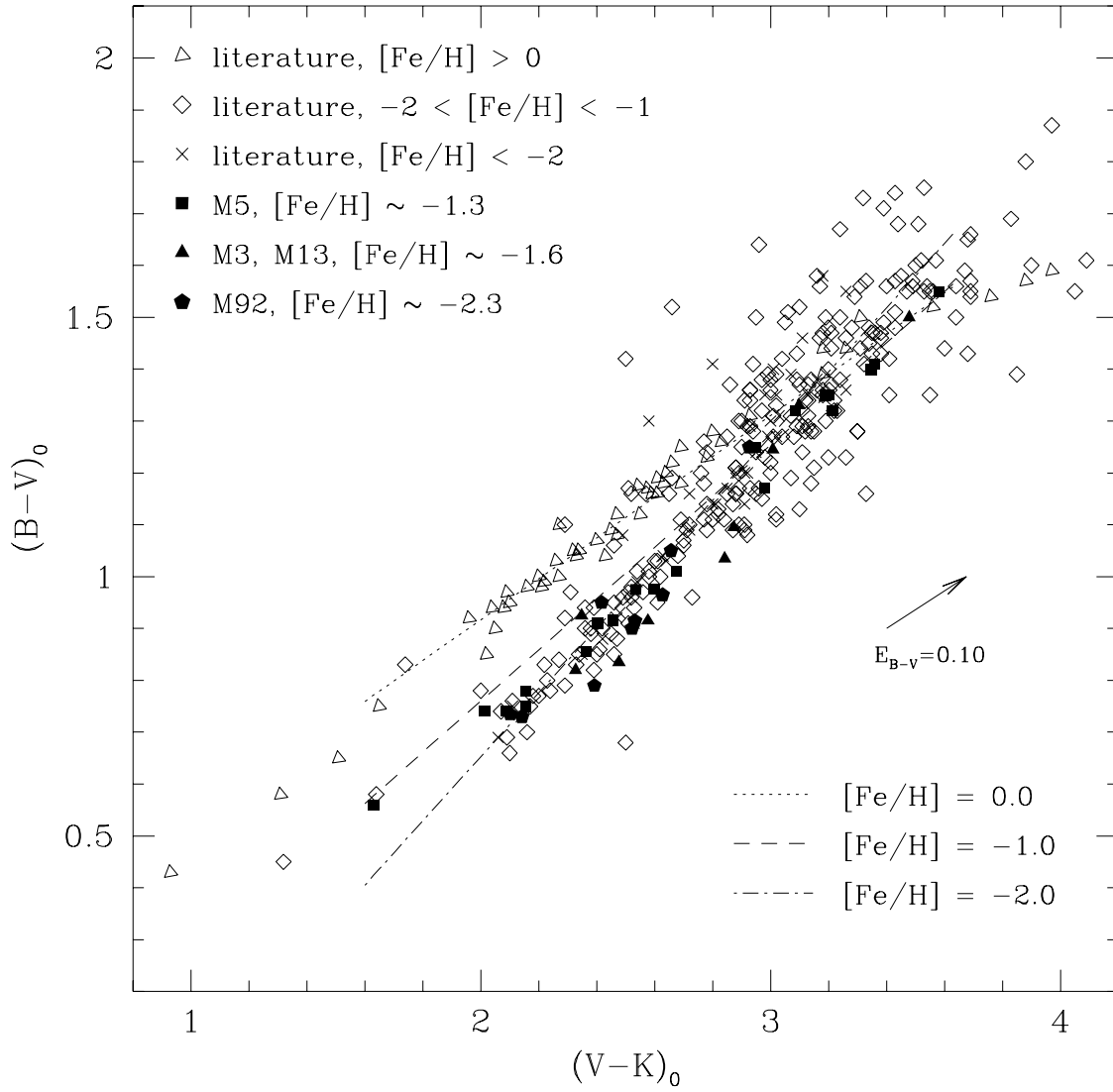


Fig. 3.— The color plane $(B-V)_0$ versus $(V-K)_0$. Symbols, line types, and reddening vector as in Fig. 2. The metallicity dependence (cf. equation (8)) is clearly visible. Fits for all $[\text{Fe}/\text{H}]$ values seem to intersect at $(V-K)_0 \sim 3$.

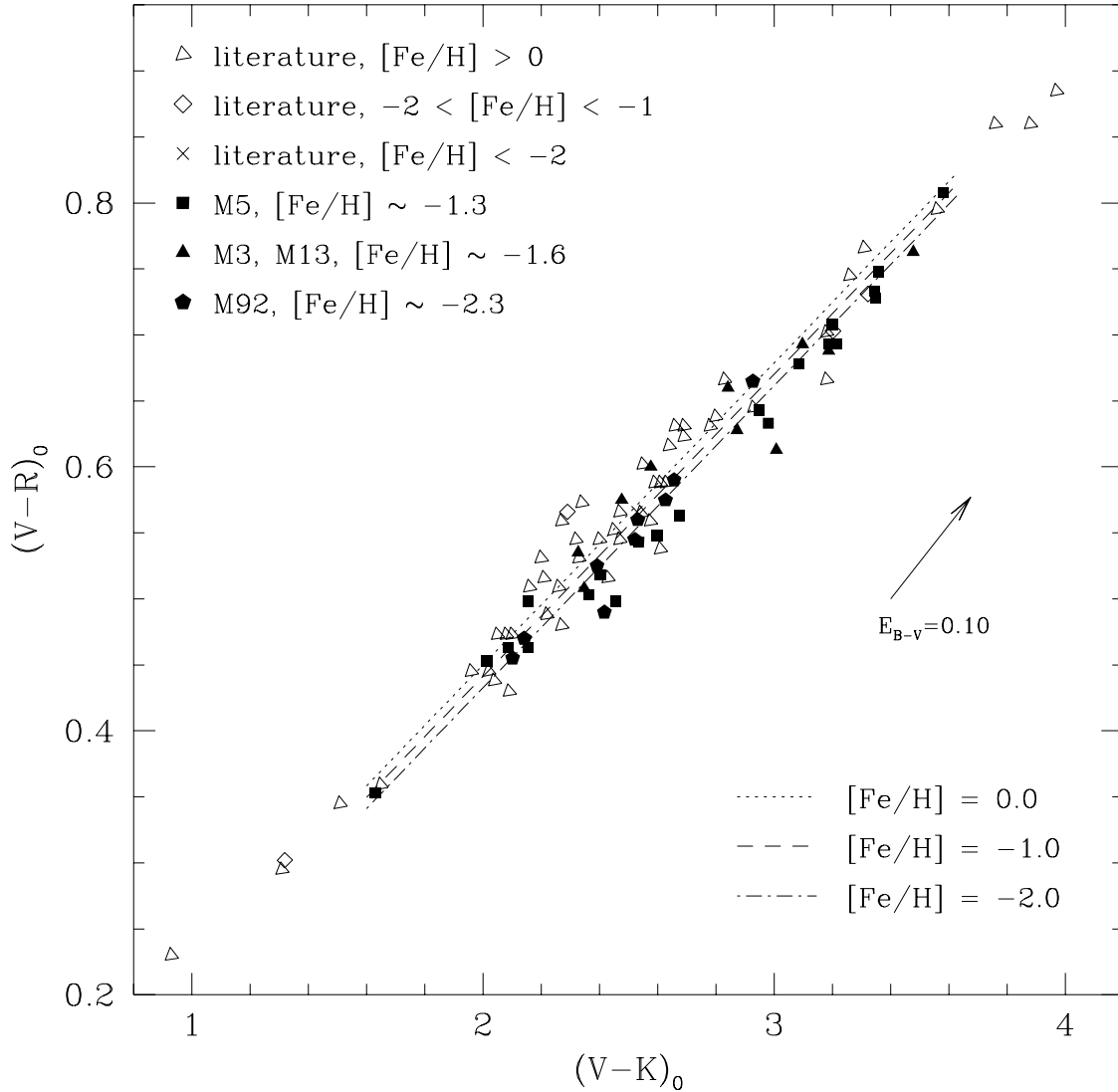


Fig. 4.— The color plane $(V - R)_0$ versus $(V - K)_0$. Symbols, line types, and reddening vector as in Fig. 2. There are very few metal-poor stars available from the literature for this color plane. Only little evidence is visible for a metallicity trend even though stars with more than a factor of 100 difference in abundance are plotted. Note, however, the subtle divergence of the $(V - R)_0$ sequence for $2 < (V - K)_0 < 3$. For the analytical form of the fits seen in this figure, see equation (9).

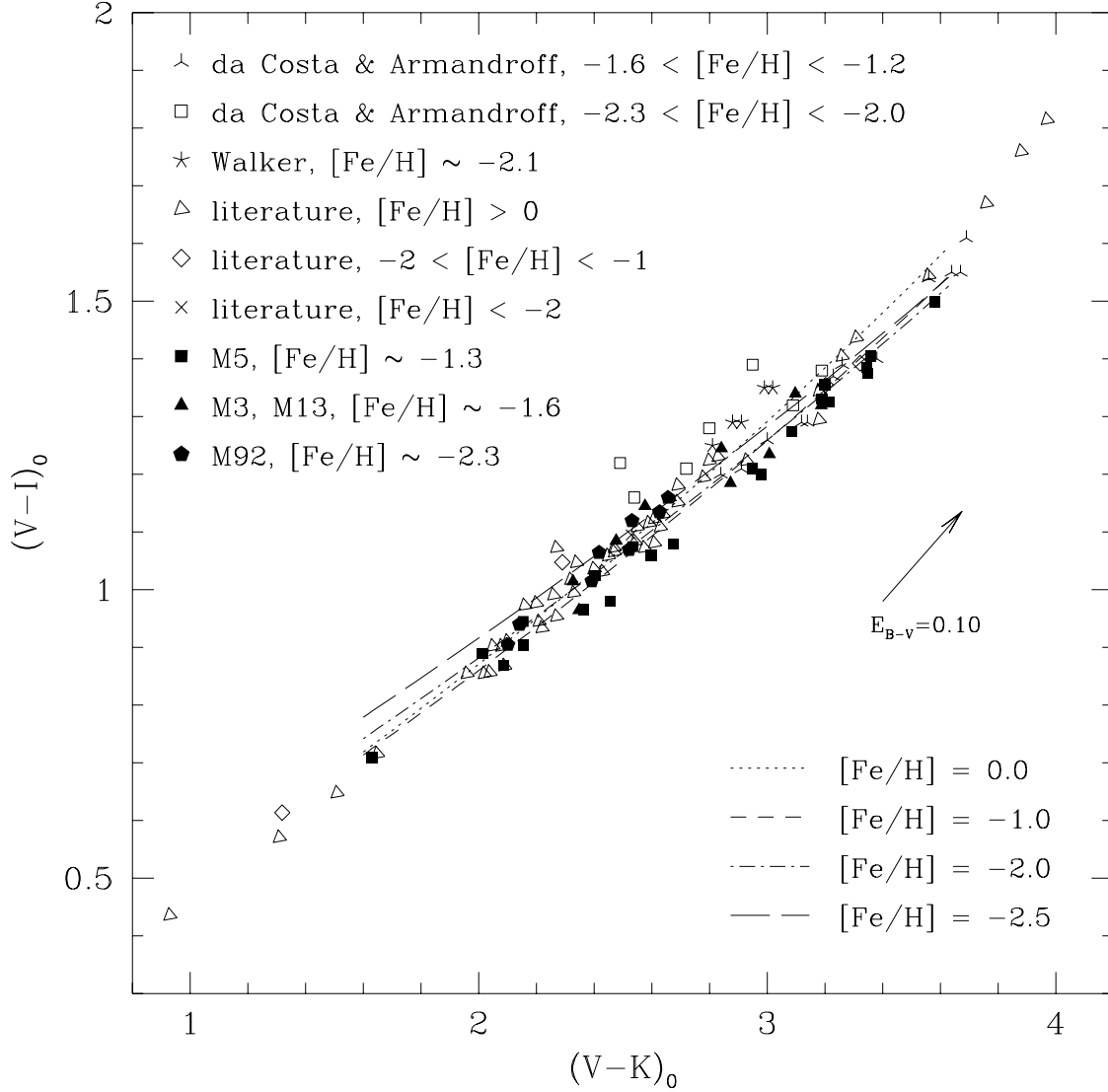


Fig. 5.— The color plane $(V - I)_0$ versus $(V - K)_0$. Symbols, line types, and reddening vector as in Fig. 2, with three extra symbol types for the main sources of literature $(V - I)_0$ data: Walker (1994) for M68, and da Costa & Armandroff (1990) for NGC 6397, M15, NGC 1851, and NGC 6752. The three high-lying da Costa & Armandroff points all belong to cluster M15 ($[\text{Fe}/\text{H}] = -2.22$) (Harris, 1996). Note the interesting behavior of $(V - I)_0$ with $[\text{Fe}/\text{H}]$ (cf. equation (10)).

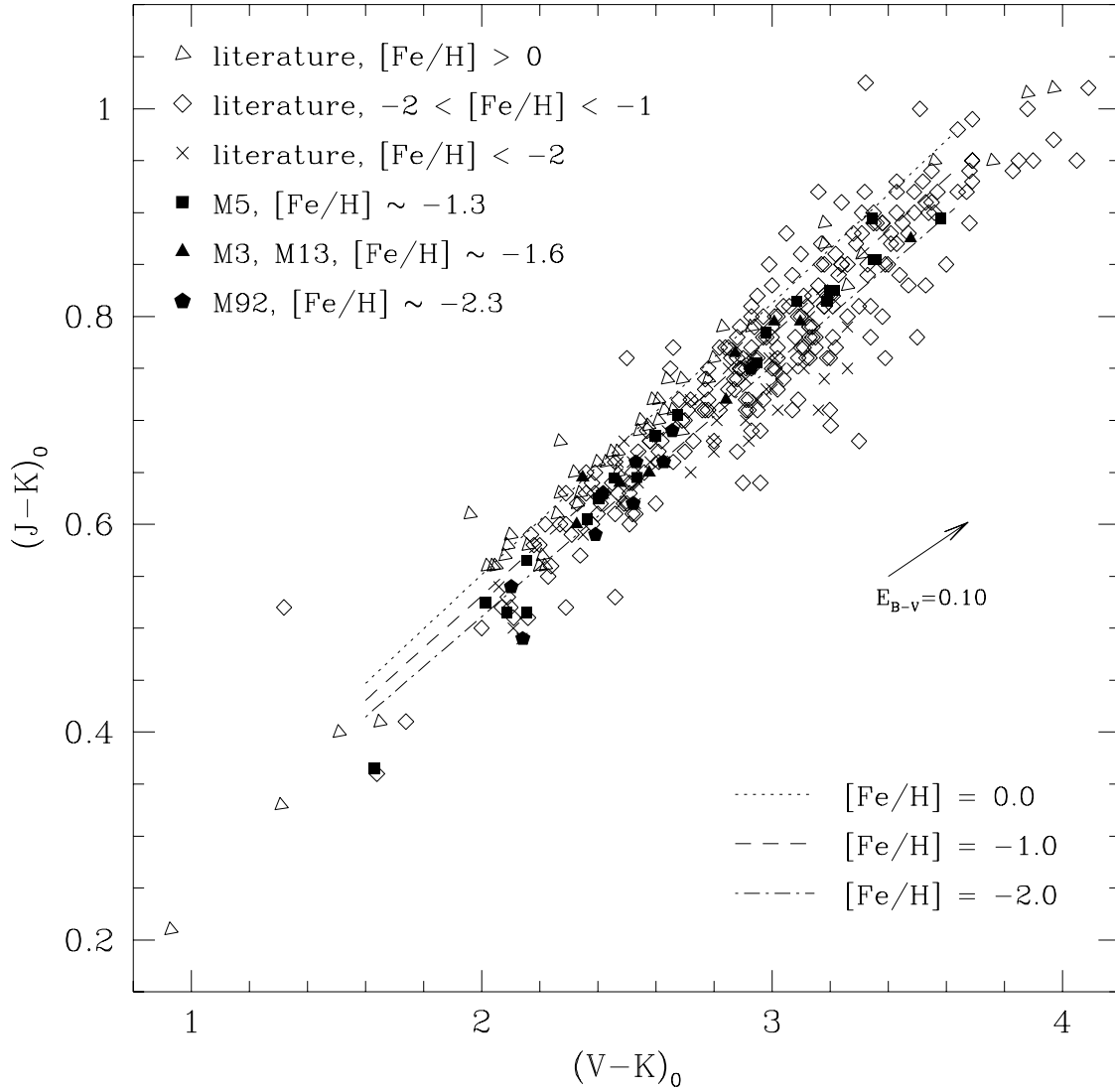


Fig. 6.— The color plane $(J - K)_0$ versus $(V - K)_0$. Symbols, line types, and reddening vector as in Fig. 2. We find a statistically significant dependence upon metallicity (see text and equation (11)).

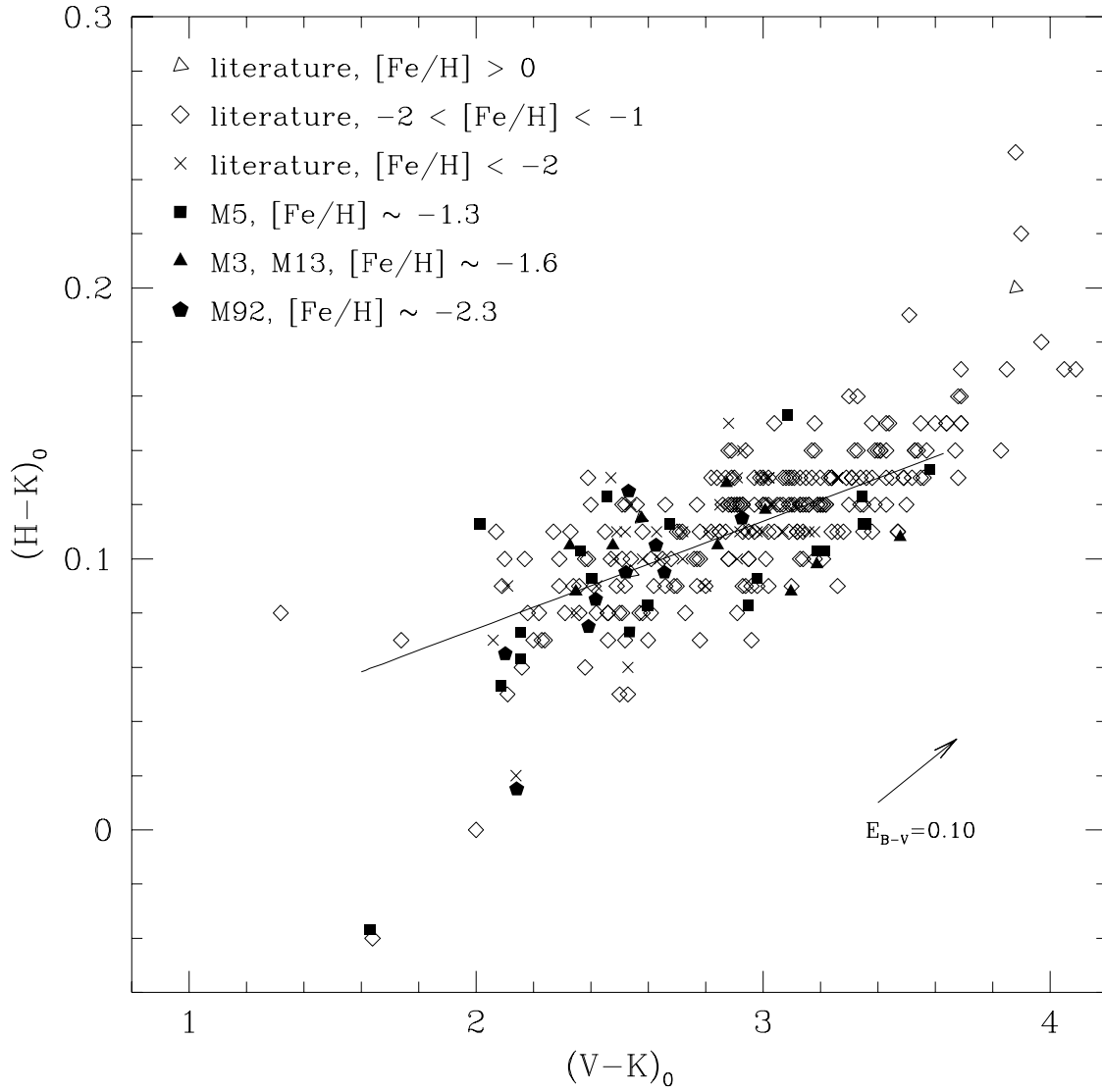


Fig. 7.— The color plane $(H - K)_0$ versus $(V - K)_0$. Symbols and reddening vector as in Fig. 2. Note that the $(H - K)_0$ range is small compared to its observational error. We supply the metallicity independent fit for the data (cf. equation (12)).